A JOINT IEEE/OSA PUBLICATION

Journal of LIGHTWAVE TECHNOLOGY

MMM 2003 VOLUME 21 NUMBER 11 JLTEDG (ISSN 0733-8724)

PAPER

Nonblocking All-Optical Cross Connect Based on Regenerative All-Optical Wavelength Converter in a Transparent Demonstration Over 42 Nodes and 16800 km

Juerg Leuthold, Roland Ryf, Drew N. Maywar, Steven Cabot, James Jaques, and S. S. Patel

***Abstract*—A red-shift optical filter all-optical wavelength converter compatible to all-optical WDM networks is introduced and demonstrated at 40 and 10 Gb/s. The wavelength converter provides reshaping and can act as a power equalizer. We use the device to overcome wavelength blocking in a looped-fiber network demonstration equivalent to 42 cross-connect switches and a 16800 km transmission distance.**

***Index Terms*—All-optical, communication system routing, nonlinear optics, optical communication, optical communication equipment, optical fiber communication, optical filters, semiconductor optical amplifiers.**

I. Introduction

TRANSPARENT networks are expected to offer cost advantages by sending a signal from source to destination and thereby eliminating some expensive receiver/ transmitters at network nodes [1]–[3]. However, if channels are mapped from one port to another that already guide a signal with the same wavelength, wavelength blocking becomes an issue. Such wavelength blocking can be overcome with wavelength translator units. These translators might be based on power-consuming, large footprint optical-to-electrical-to-optical (OEO) translator units or on all-optical wavelength converters (AOWC). AOWC are relatively new and must not only be less expensive, but also prove to be simple and have regenerative characteristics. In an OEO translator unit regeneration performance is a matter of the quality of the receiver, transmitter and electronics. However, regeneration in AOWC is a matter of the underlying configuration and materials. And indeed, AOWCs with retiming and reshaping have already demonstrated regenerative transmission over one million kilometers [4]. Yet, schemes that only perform reshaping are much cheaper and simpler and may be sufficient. With such schemes cascading over multiple loops has already been performed [5]–[7].

In this paper we introduce a new regenerative all-optical wavelength converter that is compatible with multiplexing schemes used in existing switch fabrics and optical cross connects (OXC). The AOWC is comprised of a CW source, a coupler, one or two semiconductor optical amplifiers and a red-shift optical filter (RSOF). Features of the regenerative all-optical wavelength converter are as follows

- Since our RSOF is periodic with the ITU grid, a single filter performs wavelength conversion on all WDM channels, making it a multiwavelength regenerative approach. Also, the filter is transparent for through channels yet still performs the necessary transformation on the channels undergoing wavelength conversion.
- Input powers needed to perform wavelength conversion are low and thus there is no single-channel amplification needed for the CW or input-signal within the switch fabric.
- The RSOF based wavelength converter is transparent with respect to protocols and bit rates. Yet, it is not amplitude transparent – instead it is amplitude regenerative.
- In particular it is shown that strong reshaping regeneration with respect to pulse broadening, optical signal-to-noise ratio (OSNR) suppression and extinction ratio improvement is achieved with this scheme enabling transmission over 16 800 km or as much as 42 network nodes in a network demonstration with three active channels.
- Finally, but very significantly, the scheme enables simultaneous power equalization of the wavelength converted channels when a simple feedback loop is used.

The paper is organized as follows. We first discuss the AOWC in Section II, followed by Section III where we describe how the wavelength converter can be implemented into a network node and discuss the loop setup. It is shown that the AOWC of Section II is compatible with existing cross connect setups. Results of the three-channel network experiment and characterization of the regenerative behavior of the wavelength converter are given in Section IV. The paper is concluded in Section V.

II. AOWC Based on Red-Shift Optical Filtering

The all-optical wavelength converter is depicted in Fig. 1(a). It consists of a CW source, a coupler and one or two semiconductor optical amplifiers (SOAs). The first amplifier is a conventional SOA while the second is a linear optical amplifier (LOA) [8]. The first SOA provides the necessary nonlinear response for wavelength conversion. The second amplifier is used to provide gain equalization by setting its current to provide equal output-power in all wavelength-converted channels of the cross connect. This way the output power of the converted channel can

Manuscript received February 25, 2003; revised May 8, 2003.

The authors are with the Lucent Technologies, Bell Labs, Holmdel, NJ 07733 USA

Digital Object Identifier 10.1109/JLT.2003.819140

be tuned by at least 8 dB when changing the current of the LOA. It is anticipated that the SOA and LOA could be integrated into a single SOA or a two-section SOA (nonlinear SOA followed by a booster SOA). At the output of the wavelength converter a waveguide grating router (WGR) filter is used to separate the input signal from the CW signal and to multiplex (MUX) other channels of the cross connect into a common output fiber. A flat top interleaver is placed at the output. We will see later, that this filter transforms the signals to be wavelength converted.

The wavelength conversion scheme is based on red-shift optical filtering (RSOF) of the chirped CW signal at the output of the SOAs [9], working as follows. In the absence of an input signal, only the CW signal (dashed line in Fig. 1(b)) is coupled into the SOA and amplified. The amplified CW signal is then guided into the WGR and the interleaver at the output. However, the passband of the interleaver (dash-dotted line in Fig. 1(b)) is tuned to suppress the CW signal such that no signal is guided into the output. If an input data signal is launched into the SOA, the CW signal is chirped initially toward longer wavelengths (red chirp) followed by chirp toward the shorter wavelength (blue chirp) as the power of the data signal decays [dotted line in Fig. 1(b)]. While the WGR and interleaver will allow the red-shifted spectrum to pass, the blue-shifted portion will be suppressed. Thus the WGR and the interleaver form the RSOF, that spectrally shapes and forms the new wavelength converted signal [solid line in Fig. 1(b)]. The red-shifted spectral components have been selected rather than the blue shifted spectral components because they are governed by the fast carrier depletion effects rather than the somewhat slower carrier relaxation effects of the blue spectral components. However, if the nonlinear media is reasonably fast, a blue-shift optical filtering (BSOF) scheme will work well. The copropagating input signal needs to be suppressed as well. It is filtered by the waveguide grating router (WGR) multiplexer that is already part of the RSOF. Note, that in our case, only one RSOF is needed for performing multiple WDM channel wavelength conversion, since both the WGR and interleaver are ITU grid compatible.

Eye diagrams showing wavelength conversion at 40 and 10 Gb/s are depicted in Fig. 1(c). Clear and open eyes of the converted signals demonstrate bit-rate transparency of the scheme for signals up to 40 Gb/s and potentially beyond. The eye diagrams of the converted signals show visibly less noise in the spaces, i.e., "zeros." The signal qualities have been determined with a bit-error rate (BER) tester and pseudorandom bit patterns of length $2^{31}-1$. The two experiments at different bit rates were performed under identical conditions (83 GHz passband interleaver) and set-up parameters (CW signal provided by external cavity laser detuned by 47 GHz from 1 dB interleaver passband edge), input-signal powers ($P_{\rm in} = 9\ {\rm dBm}$ in fiber before 50:50 coupler) and input-signal wavelengths ($\lambda_{\rm in} = 1560\ {\rm nm}$) and CW-signal power ($P_{\rm CW} = 10\ {\rm dBm}$ in fiber before 50:50 coupler) and CW signal wavelength ($\lambda_{\rm CW} = 1556.70\ {\rm nm}$). For performing the experiment, we only replaced the 40 Gb/s 33% RZ source by a 33% 10 GB/s RZ source, generated through an electroabsorption modulator pulse carver followed by a Mach-Zehnder Lithium Niobate for data encoding.

A limitation to the bit-rate transparency at the highest speed is due to the finite carrier relaxation times of the SOA and the passband of the interleaver [10]. In our case, the interleaver passband is 83 GHz which limits operation to 40 Gb/s. At lower bit rates the limitation is due to the filter passband and the power required to induce chirp. The induced chirp decreases with decreasing bit rates. The best conversion efficiency is expected for an almost rectangular shaped filter that allows good blocking of the CW signal and provides transparency to small chirps.

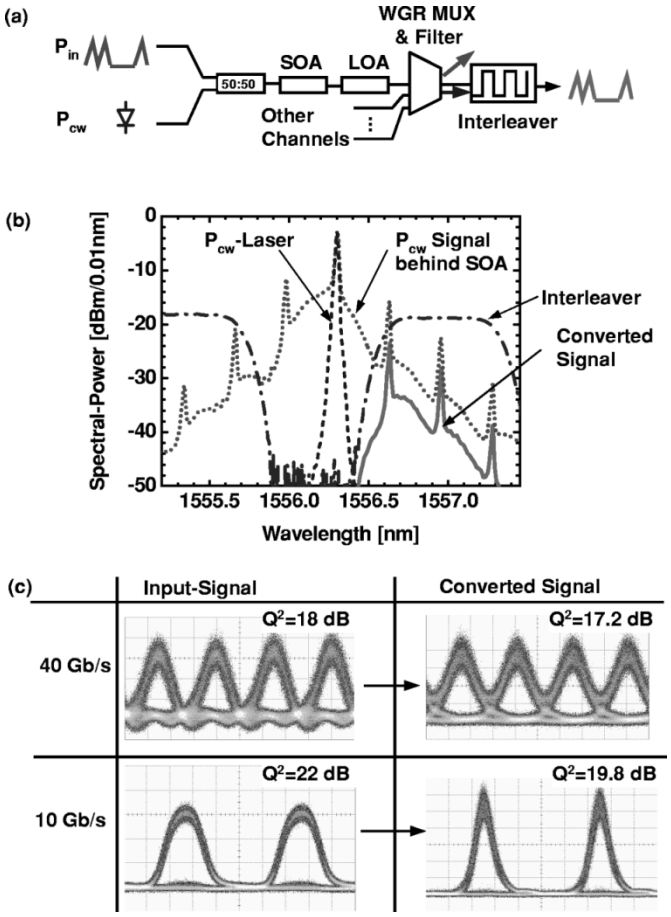

Fig. 1. (a) Wavelength converter comprising a coupler, an SOA section, a red-shift optical filter (RSOF) composed of a WGR multiplexer and a channel interleaver. (b) Spectrum of the CW signal (dashed), the modulated CW signal behind the SOA (dotted) and the wavelength converted signal $P_{\rm cv}$ (solid) as obtained by the interleaver filter (dash-dotted). (c) Eye diagrams and signal qualities of 40 Gb/s and 10 Gb/s input signals and wavelength converted signals. The 40 and 10 Gb/ experiments were performed under identical conditions in order to demonstrate real bit-rate transparency.

Tolerance to input-power variations has been assessed at 10 Gb/s. All characterizations were performed with a single tensile strained bulk SOA operated with 250 mA.

Tolerance to input-power variations and CW-frequency offsets with respect to the interleaver edge has been assessed at 10 Gb/s. All characterizations have been performed with only a single SOA in the setup of Fig. 1(a). The omission of the LOA will lead to a reduced conversion efficiency but will otherwise not change the characteristics, since the LOA mainly provides linear gain.

The effect of a variation of the input-power for three different CW-signal powers at 0, 4 and 8 dBm are shown in Fig. 2(a). The first plot shows the dynamic input-power range. A 12.5 dB dynamic input-power range with signal qualities better than 15.6

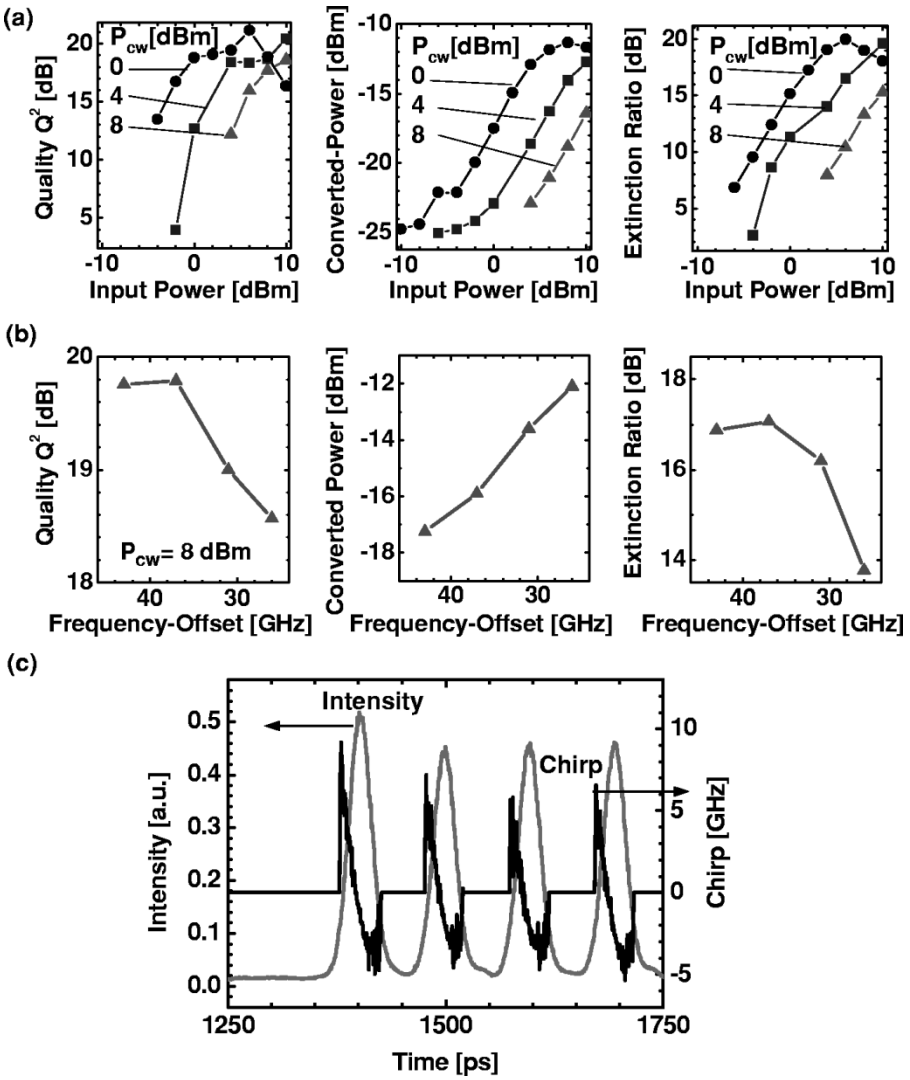

Fig. 2. Wavelength conversion characteristics of the filter scheme at 10 Gb/s as obtained from a single SOA. (a) Dependence of signal quality Q^2, conversion efficiency and extinction ratio on input signal power and for P_{CW} laser powers of 0, 4 and 8 dBm. (b) Tolerance of RSOF scheme toward detuning of input-signal wavelength with respect to the edge of the interleaver. (c) Intensity and chirp characteristic of wavelength converted pulse.

dB has been measured, which – except for [11] – is to the best of our knowledge the best ever reported value. The conversion efficiency is shown in the second plot. The transfer function of the input to the output power shows the typical S-shape of regenerative devices [12]. The last plot shows improvement of extinction ratios with increasing input-power. A definition of the extinction ratio is given later. Extinction ratios up to 19 dB were found. Yet, extinction ratios better than 14 dB are already found for input-powers as low as 0 dBm.

Tolerance to detuning of the CW-signal wavelength with respect to the 1 dB interleaver edge was tested in Fig. 2(b). In this experiment the CW center frequency was gradually moved toward the interleaver passband – starting with an offset of 47 GHz and stopping at an offset of 26 GHz. While the signal quality decreases only little when moving the CW frequency toward the red-shifted interleaver passband, the conversion efficiency increases by as much as 5 dB. A further shift toward the filter will result in excessive extinction ratio degradation.

Since the device exploits chirp for performing wavelength conversion, the chirp of the wavelength converted signal is of special interest – in particular in view of telecommunications transmission applications. A measurement of the chirp for a "01 111" signal sequence is displayed in Fig. 2(c). The wavelength converted signals show a linear red-chirp in all pulses. This linear and predictable chirp behavior makes it very easy to compensate dispersion with conventional dispersion compensated fiber.

Fig. 2(c) additionally indicates that the scheme is sufficiently stable for burst mode operation. The "01 111" sequences follows a long sequences of spaces and only the first bit of the "1111" pattern shows a very small pattern dependence. All subsequent mark "1" have the same intensity level. This is an attractive characteristic as desired by some bursty IP centric transmission protocols.

III. Nonblocking Cross Connect and Loop Setup

To demonstrate the compatibility of the AOWC within a cross connect and to show the regenerative performance of the AOWC we have set up a recirculating loop equivalent to

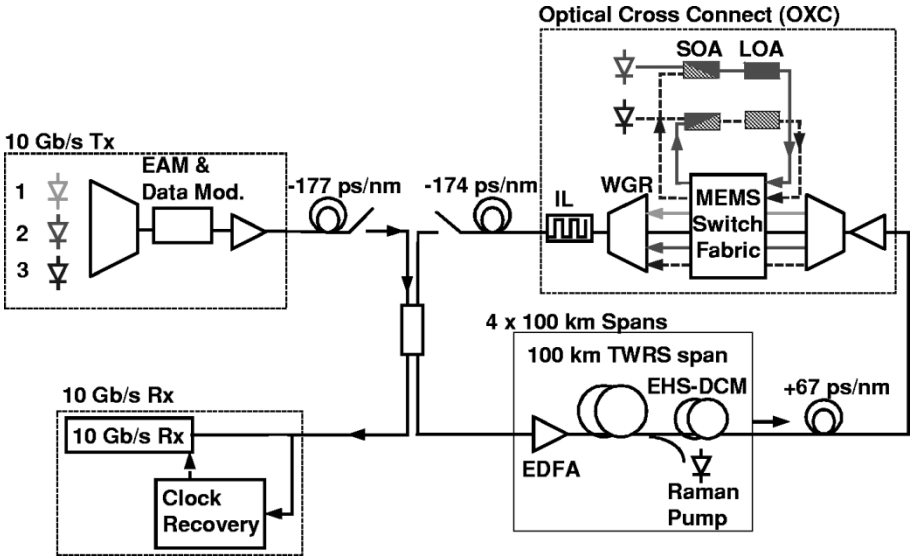

Fig. 3. Loop setup and cross connect to mimic a transparent meshed network.

having an OXC every 400 km. We mimic a meshed network with a through channel and two channels that are dropped, interchanged, and added at every node. That is, channel 2 is dropped and mapped onto channel 3 and channel 3 is dropped and mapped onto channel 2. Since the two channels are interchanged, wavelength conversion is needed to avoid wavelength blocking.

The loop setup is shown in Fig. 3. The transmitter consists of the three DFB lasers emitting at 1549.7, 1551.3, and 1552.9 nm; all are guided through the same electroabsorption modulator (EAM) that serves as a pulse carver. 10 Gb/s return-to-zero (RZ) data with a PRBS of $2^{31}-1$ are then encoded onto the signals in a $\mathrm{LiNbO_3}$ modulator. The receiver consists of a clock-recovery module and an 8-GHz bandwidth receiver and a BER tester. The transmission span consists of four 100-km spans of TrueWave® Reduced Slope (TWRS) nonzero dispersion fiber and DCF fiber for dispersion compensation. EDFAs and backward pumped Raman amplification are used to compensate the 21-dB span losses. Precompensation before the loop and a tunable dispersion compensator before the OXC have been used to reset the dispersion in every loop, respectively.

It is important to note, that a cross connect recirculating loop experiment is fundamentally different from a long-haul transmission experiment. In the long haul transmission experiment, the dispersion map, span lengths and sources are optimized for transmission over a single long point-to-point link [13], [14]. This means, that an optimized dispersion map for the particular length, short transmission spans and chirp-free sources are preferentially used. In contrast, in a recirculating all-optical cross-connect experiment, the dispersion map must be reset at every cross connect node. This way signals can be dropped, mapped to other ports or bypass the switch and new signals can be added at every node. Unfortunately, resetting of the dispersion typically comes at the price of higher nonlinear distortion which degrades transmission performance. An additional cross-connect penalty results from filter concatenation. WGR filters with finite signal passbands at the input and output of the cross connect suppress part of the signal tones and may adversely affect the signal. This becomes a limiting issue if filters are concatenated [15], [16].

A particular challenge in our setup is having signals from two sources, each with different chirp characteristics. First of all we have the red chirped signals generated by the EAM. Second the wavelength-converted signals with the small red chirp. Thus, the tunable dispersion compensator at the cross connect needed to be set for the optimum operation point of either of them. In this experiment the tunable dispersion compensator was set for optimum transmission of the through-channel generated by the EAM. The channels undergoing wavelength conversion are tolerant to dispersion mismatch, since chirp is reset in the process of all-optical wavelength conversion.

The optical cross-connect is schematically shown in Fig. 3. It consists of a flat-top 200 GHz channel spaced demultiplexing WGR (DEMUX, 5.2-dB loss) at the input to split signals according to wavelength. The inputs are then guided into a MEMS based switch fabric. The switch fabric allows through channels to pass with low losses of 2 dB [17]. Any channel can be dropped, added or mapped to any port by means of the switch fabric. Channels that are mapped onto a new port and those that need wavelength conversion are first guided onto a separate port having a wavelength converter set to the needed wavelength and then guided back into the switch fabric. From there they are mapped onto the desired output port. The converted signals are then routed to the multiplexing WGR (MUX, 5.4-dB loss). The final-stage 100-to-200 GHz interleaver is placed at the output of the OXC (2-dB loss). Input signal powers of the channels to be wavelength converted were 0.0 dBm into the SOA when performing wavelength conversion from 1551.2 to 1552.9 nm and 3.5 dBm when converting from wavelengths 1552.9 to 1551.2 nm, respectively. The corresponding CW powers were $+2.9$ and $+5.3\ \mathrm{dBm}$, respectively. All powers were measured in the fiber before the 50:50 splitter. I.e. the actual power guided into the SOA were -3.5 and $-0.5\ \mathrm{dBm}$. The signal power levels of the converted and the through channel were $-14\ \mathrm{dBm}$ at the output of the cross-connect. Through channels that are not wavelength converted pass the interleaver.

Note, that the output multiplexer (here a WGR) and the interleaver are already part of most cross connects, where they enable wavelength multiplexing. At the same time they form the RSOF needed for performing wavelength conversion. As wavelength conversion filters they suppress the undesired input signal and are the red-shift wavelength conversion filter for channels undergoing wavelength conversion.

IV. Results

We launched all three 10-Gb/s signals simultaneously into the system. The cross-connect was set such that port 1 was the through-channel while ports 2 and 3 were dropped. To mimic an all-optical network we interchanged the channels and fed them back into the OADM. For example, in the first loop channel 2 was dropped, wavelength converted and mapped onto the port of channel 3 and channel 3 was dropped, wavelength converted and mapped to the port of channel 2. In the next loop they were mapped back to the initial ports.

We characterized signals after 400, 1200, 2000, 2800, 4400, 8400, 11 200, 16 800 km transmission distances. The quality or Q^2-value of the through-channel 1 outperformed the wavelength converted add/drop channels for short transmission distances. However, after 2000 km, the signal quality of the through-channel dropped from 21.8 to 16.2 dB. In contrast, the quality of the add/drop channels with wavelength conversion showed Q^2-values around 19 dB at distances up to 8800 km. Timing-jitter degradation then decreased the signal quality. After 16 800 km the quality of the signal was still around 18 dB. Signal quality versus distances are given in Fig. 4(a). V-plots showing the BER versus the decision threshold are depicted in Fig. 4(b). We used an inverting receiver such that the negative rails show the bit errors of the marks "1s" and the positive rails show the bit errors of the spaces "0." There is an initial degradation between the back-to-back measurement at 0 km (square) and the wavelength converted signal after 400 km (circles). However, there is hardly any further degradation when transmitting the signal over subsequent loops. And indeed, after 16 800 km one can only see a small change of the slope in the rail of the "1" and hardly any change in the slope of the "0" rails.

The eye diagrams of the 10 GB/s signals after 1, 5, 28 and 42 loops are shown in Fig. 5. The eye diagrams of the through-channel are shown at the 1st and 5th loop. The eye diagrams of the channels that undergo wavelength conversion are also shown after 28 and 42 circulations. Open eyes are found for the converted and the through-channels up to 2000 km. Yet, the through-channel shows significant degradation after 2000 km. In contrast, the channels that undergo all-optical wavelength conversion show an open eye up to transmission distances of 42 loops corresponding to 16 800 km.

A systematic discussion of all-optical regeneration and its different aspects was given elsewhere [12]. Here we discuss the regenerative potential of the wavelength converter with respect to pulse broadening, optical signal-to-noise (OSNR) degradation, extinction ratio, contrast ratio and timing jitter.

Information on regeneration and pulse broadening can be obtained from the eye diagrams. While the through-channel shows significant pulse broadening after the 5th loop, the pulse of the wavelength converted channels is maintained. The only visible degradation is presumably due to timing-jitter accumulation.

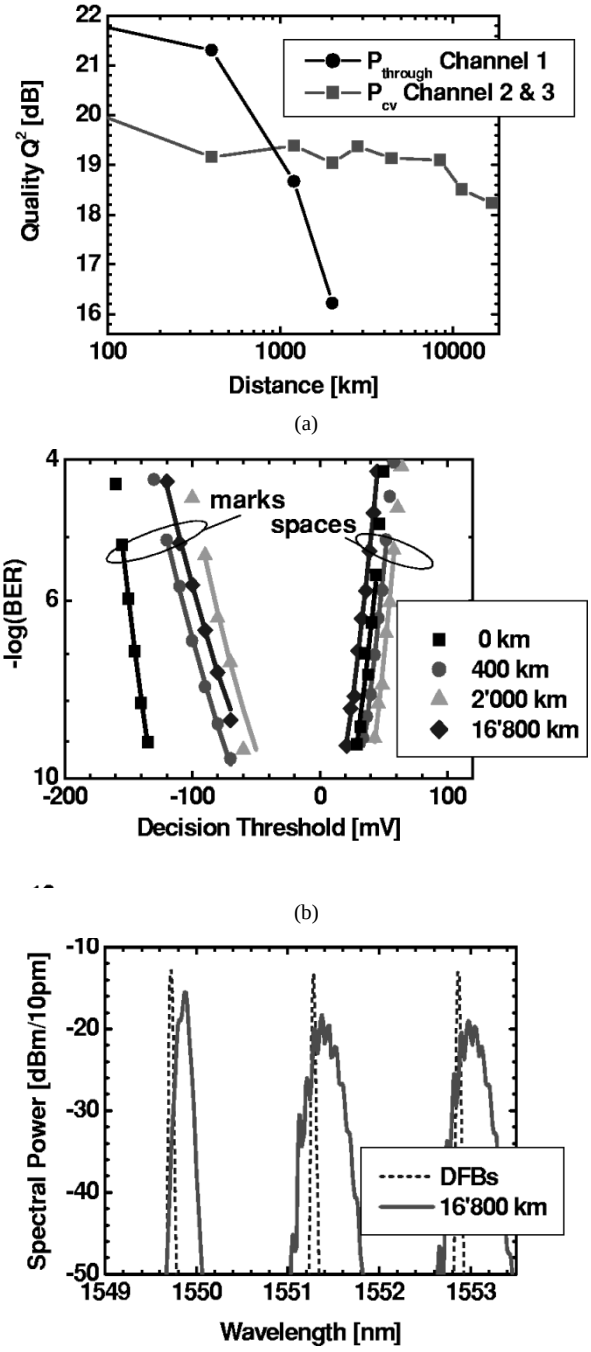

Fig. 4. (a) Q^2-values versus distance for wavelength converted add/drop channels and for through channels. (b) Voltage versus BER plots at various distances. (c) Spectrum of the DFB lasers at the input and spectrum after 16'800 km. The spectra of the two channels undergoing wavelength conversion are almost identical to the spectra after 400 km, whereas the spectrum of the through channel is severely degraded.

OSNR degradation is successfully mitigated as well. Amplified spontaneous emission (ASE) accumulation which leads to noise in the spaces "0s" and increased amplitude fluctuations in the marks "1s" is visible in the eye diagram of the through-channel after 5 loops. The wavelength-converted channel however shows no sign of noise accumulation in the "0s" up to the 42nd loop and no broadening of the amplitude in

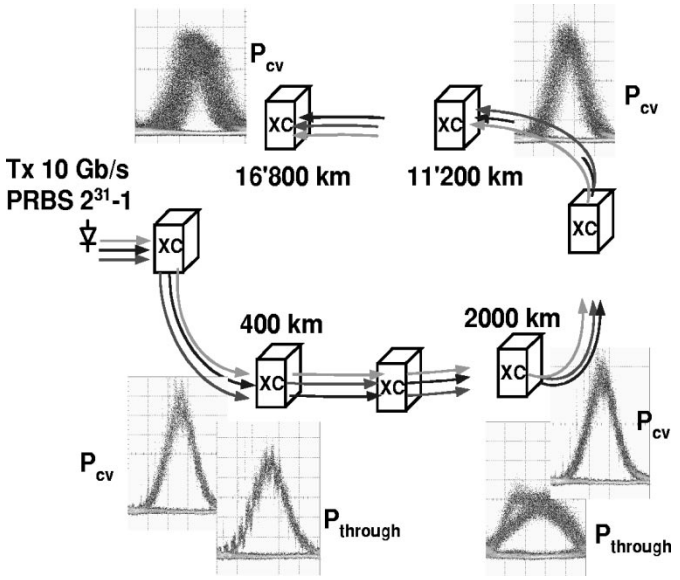

Fig. 5. Eye diagrams of the through P_{through} and converted channel P_{cv} after 400, 2000, and the converted channel after 11 200 and 16 800 km.

the mark levels due to signal-ASE beating up to the fifth loop and beyond. Timing jitter accumulation makes it difficult to see mitigation of amplitude fluctuations in the eye diagrams after the 28nd and 42th loop. However, the V-plots from Fig. 4(b) show, that amplitude fluctuations are indeed successfully suppressed up to these distances. The slope of the mark rail is almost identical independent of the transmitted distance.

To assess the strength of the regenerative characteristics of the wavelength converter further, we separately characterized the extinction ratio, contrast ratio, and timing jitter of the signal at different transmission distances. Measurements were performed by feeding the optically preamplified signal into a photodiode having a 55-GHz bandwidth and evaluating the signal levels with a calibrated Agilent oscilloscope. In Fig. 6 we show an eye diagram at 8400 km of one of the channels undergoing wavelength conversion. In this eye diagram the extinction ratio is defined as the ratio of the mean value of the "one" level and the mean value of the "zero" level. The contrast ratio is a figure of merit for the intrachannel crosstalk, defined as the mean of the "one"-level divided by the mean of the peak in the valley between two bits after removal of the mean "zero"-level. Finally, we use the peak-to-peak jitter at the 50% signal level measured as the maximum jitter in the positive transient of the signal.

The evolution of the extinction ratio of the through-channel and the channels undergoing wavelength conversion is given in Fig. 7(a). While the extinction ratio of the through-channel degrades quickly, there is no sign of extinction ratio degradation for the channels undergoing wavelength conversion. Indeed, the extinction ratio improves after wavelength conversion. The high extinction ratio of 17 dB is a result of the extinction of the CW signal provided by the interleaver filter shown in Fig. 1(b).

A similar characteristic is found for the evolution of the contrast ratio along the transmission distance. The contrast ratio of the channel undergoing wavelength conversion hardly degrades, whereas the contrast ratio of the through-channel degrades quickly, as shown in Fig. 7(b).

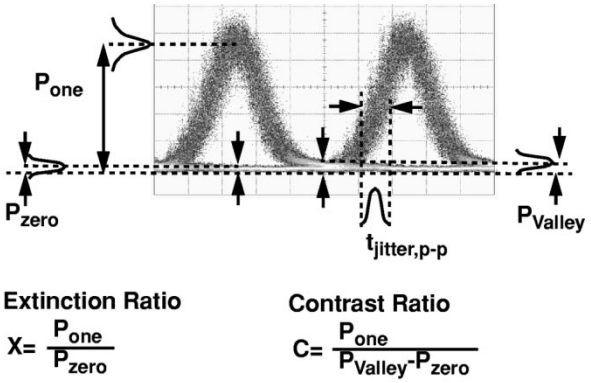

Fig. 6. Eye diagram of the converted channel after 8400 km and definition of extinction ratio, contrast ratio, and peak-to-peak timing jitter as used later.

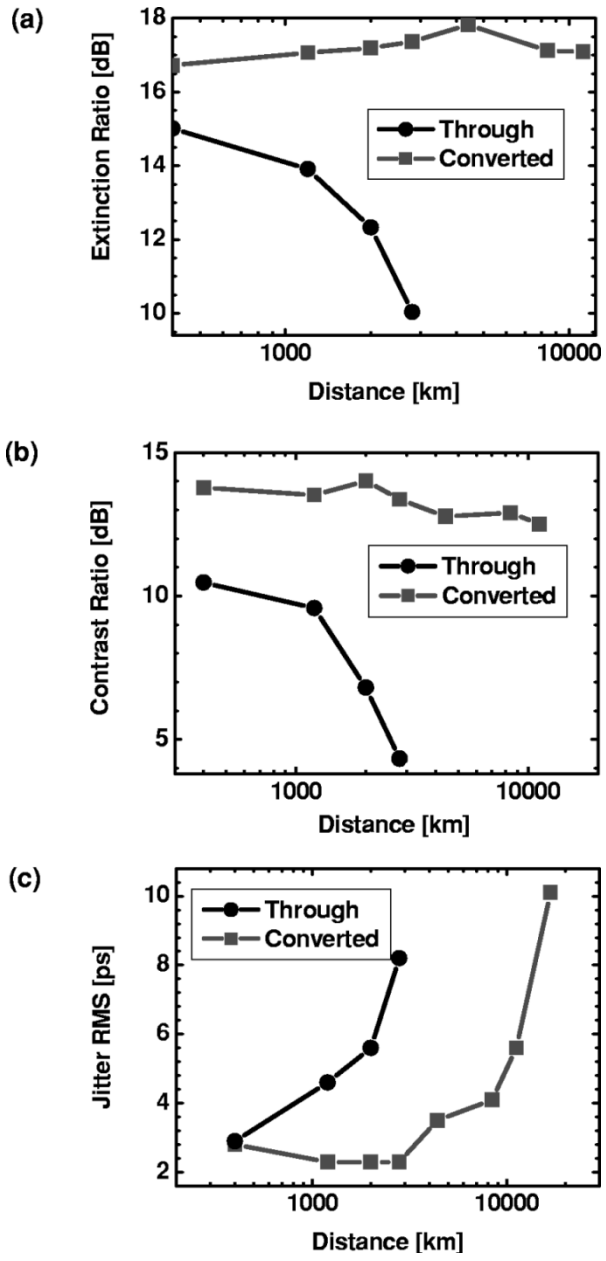

Fig. 7. (a) Extinction ratio. (b) Contrast ratio. (c) Peak-to-peak timing-jitter evolution of the through and converted channel with distance.

The peak-to-peak timing-jitter accumulation is shown in Fig. 7(c). Timing jitter accumulates as the signals propagate along the fiber and reaches as much as 10 ps when BERs increase. The timing jitter of the through-channel increases earlier as the result of pulse broadening, amplitude fluctuations and timing jitter. However, when measuring the peak-to-peak jitter of the wavelength converted channels the only contribution is due to real timing jitter, since the other effects are mitigated by the regenerative wavelength converter.

V. Conclusion

A new wavelength converter concept compatible with existing switch architectures has been demonstrated. Q^2-values of 10-Gb/s signals after 16 800 km and 42 wavelength conversions are better than 18 dB. The new scheme successfully regenerates signals and mitigates pulse broadening, signal-to-noise ratio degradation and extinction ratio degradation.

References

[1] A. Jourdan, G. Soulage, S. Artigaud, K. Wunstel, P. Doussiere, M. Bachman, J. Da Loura, F. Bruyere, and M. Sotom, "WDM networking experiment including all-optical crossconnect cascade and transmission over 320 km G.652 fiber at up to 10 Gbit/s," in *ECOC'1996*, vol. 4, Sept. 1996, pp. 123–126.

[2] R. J. S. Pedersen, B. F. Jorgensen, B. Mikkelsen, M. Nissov, K. E. Stubkjaer, K. Wunstel, K. Daub, E. Lach, G. Laube, W. Idler, M. Schilling, P. Doussiere, and F. Pommerau, "Cascading of a nonblocking WDM cross-connect based on all-optical wavelength converters for routing and wavelength slot interchanging," *Electron. Lett.*, vol. 33, no. 19, pp. 1647–1648, Sept. 1997.

[3] J. Leuthold, R. Ryf, S. Chandrasekhar, D. T. Neilson, C. H. Joyner, and C. R. Giles, "All-optical nonblocking Terabit/s crossconnect based on low power all-optical wavelength converter and MEMS switch fabric," in Proc. Opt. Fiber Comm. Conf. OFC'2001, Anaheim, CA, Mar. 2001, pd. 16.

[4] J. Leuthold, G. Raybon, Y. Su, R. Essiambre, S. Cabot, J. Jaques, and M. Kauer, "40 Gb/s transmission and cascaded all-optical wavelength conversion over one million kilometers," *Electron. Lett.*, vol. 38, no. 16, pp. 890–892, Aug. 2002.

[5] R. J. S. Pedersen, N. Nissov, B. Mikkelsen, H. N. Poulsen, K. E. Stubkjaer, M. Gustavsson, W. van Berlo, and M. Janson, "Transmission through a cascade of 10 all-optical interferometric wavelength converter spans at 10 Gbit/s," *Electron. Lett.*, vol. 32, no. 11, pp. 1034–1035, May 1996.

[6] O. Leclerc, G. Aubin, P. Brindal, J. Mangeney, H. Choumane, S. Barre, and J.-L. Oudar, "Demonstration of high robustness to SNR impariment in 20 Gbit/s long-haul transmission using 1.5 μm saturable absorber," *Electron. Lett.*, vol. 36, no. 23, p. 1944, Nov. 2000.

[7] D. Rouvillain, P. Brindel, F. Seguineau, I. Pierre, O. Leclerc, H. Choumane, G. Aubin, and J.-L. Oudar, "Optical 2R regenerator based on passive saturable absorber for 40 Gbit/s WDM long-haul transmissions," *Electron. Lett.*, vol. 38, no. 19, pp. 1113–1114, Sept. 2002.

[8] D. A. Francis, S. P. DiJaili, and J. D. Walker, "A single-chip linear optical amplifier," in Proc. Opt. Fiber Comm. Conf. OFC'2001, Anaheim, CA, Mar. 2001, pd. 13.

[9] D. M. Patrick and R. J. Manning, "20 Gbit/s wavelength conversion using semiconductor nonlinearity," *Electron. Lett.*, vol. 30, no. 3, pp. 252–253, Feb. 1994.

[10] H.-Y. Yu, D. Mahgerefteh, P. S. Cho, and J. Goldhar, "Optimization of the frequency response of a semiconductor optical amplifier wavelength converter using a fiber Bragg grating," *J. Lightwave Technol.*, vol. 17, pp. 308–315, Feb. 1999.

[11] J. Leuthold, D. Marom, S. Cabot, R. Ryf, P. Bernasconi, F. Baumann, J. Jaques, D. T. Neilson, and C. R. Giles, "All-optical wavelength converter based on a pulse reformatting optical filter," in Proc. Opt. Fiber Commun. Conf. (OFC'2003), Atlanta, GA, Mar. 2003, pd. 41.

[12] J. Leuthold, "Regenerative wavelength conversion," in Annual Laser and Electro Optics Society (LEOS) Meeting 2002, Glasgow, Scottland, Nov. 2002, MM1.

[13] L. F. Mollenauer, P. V. Mamyshev, and M. J. Neubelt, "Measurement of timing jitter in filtere-guided solition transmission at 10 Gbit/s and achievement of 375 Gbits/s-Mm, error free, at 12.5 and 15 Gbits/s," *Opt. Lett.*, vol. 19, no. 10, pp. 704–706, May 1994.

[14] P. S. Cho, P. Sinha, D. Mahgerefteh, and G. M. Carter, "All-optical 2R-regeneration of 10 Gb/s RZ data transmitted over 30 000 km in a dispersion-managed system using an electroabsorption modulator," in *Proc. OFC'2000*, vol. 2, Baltimore, MD, Mar. 2000, pp. 275–277.

[15] I. Tomkos, J. K. Rhee, P. Iydroose, R. Hesse, R. Vodhanel, and A. Boskovic, "Filter concatenation penalties for 10 Gb/s sources suitable for short-reach cost-effective WDM metropolitan area networks," in *Pro. ECOC'01*, vol. 3, Sept. 2001, pp. 472–473.

[16] M. Nissov, R. J. S. Pedersen, and B. F. Jorgensen, "Transmission performance through cascaded 1-nm arrayed waveguide multiplexers at 10 Gb/s," *IEEE Photon. Technol. Lett.*, vol. 9, pp. 1038–1040, July 1997.

[17] R. Ryf, J. Kim, J. P. Hickey, A. Gnauck, D. Carr, F. Pardo, C. Bolle, R. Frahm, N. Basavanhally, C. Yoh, D. Ramsey, R. Boie, R. George, J. Kraus, C. Lichtenwalner, R. Papazian, J. Gates, H. R. Shea, A. Gasparyan, V. Muratov, and J. Griffith, "1296-port MEMS transparent optical crossconnect with 2.07 petabit/s switch capacity," in *Proc. OFC'2001*, Mar. 2001, pd. 28.

Juerg Leuthold received the Master's degree in physics (dipl. Phys. ETH) in 1991 and the Ph.D. degree, both from the Swiss Federal Institute of Technology (ETH), Zürich.

From 1992 to 1998, he was with the Micro- and Optoelectronics Institute of the ETH. He has been involved in the modeling, design, and characterization of integrated devices for high-speed telecommunication applications. Since 1999, he has been with Bell Labs, Lucent Technologies, Holmdel, NJ, where he is continuing research on semiconductors for high-speed telecommunication applications and performing system experiments with high-speed components.

Roland Ryf received the B.S. degree in engineering from the Interstate University of Applied Sciences of Technology, Buchs, in 1990 and the M.S. degree in physics from the Swiss Federal Institute of Technology, Zurich, in 1995, from where he also received the Ph.D. degree in physics in 2000, working on photorefractive self-focusing and spatial solitons, holographic storage, and fast optical correlation.

Since May 2000, he has been with the Photonic Subsystems Department, Bell Labs (Lucent Technologies), Holmdel, NJ, where he focuses on the subsystem design and prototyping of large port count optical MEMs-based switches and demonstration of their of applications in transparent optical networks.

Drew N. Maywar was born in Port Huron, MI, on March 1, 1970. He received the B.S., M.S., and Ph.D. degrees in optics from the University of Rochester, Rochester, NY, in 1993, 1997, and 2000, respectively, as well as the B.A. degree with honors in religion from the same university in 1993. His Ph.D. dissertation examined the nonlinear response and all-optical processing applications of distributed feedback SOAs.

He was a Fulbright Scholar at Osaka University's Institute of Laser Engineering from 1993 to 1994, where he studied the temperature dependence of Nd:glass laser amplifiers. Under the auspices of a Dissertation Enhancement Award from the National Science Foundation, he researched all-optical memory and wavelength conversion at the University of Tokyo from 1998 to 1999. From 2000 to 2002, he was a Member of Technical Staff at Bell Laboratories, Lucent Technologies, where he co-built a DWDM Raman-amplified testbed and used it to develop and demonstrate Lucent's next-generation fiber-optic transmission system (LambdaXtreme). In 2003, he joined the Laboratory for Laser Energetics at the University of Rochester, where he is a Scientist. His research interests include laser physics, optically amplified systems, and nonlinear optics.

Steven Cabot was born in Plainfield, NJ, on May 29, 1966. He studied electrical engineering at Union County College, Cranford, and at the New Jersey Institute of Technology, Hoboken.

He joined Bell Labs, Murray Hill, NJ, in 1989 in Federal Systems where he was building undersea optical assemblies. He moved to research in 1993 where he worked on erbium fiber characterization and EDFA assemblies. In 1999, he joined the Specialty Fiber Business Unit working on high-power components and assemblies. In 2001, he joined Onetta working on novel EDFA architectures in the forward looking group. He then rejoined Bell Labs in 2002 in the Government Communication Lab.

James Jaques was born in Raleigh, NC, on December 9, 1967. He received the Bachelor's degree in physics from Virginia Tech, Blacksburg, in 1989. He received the Master's and Ph.D. degrees in particle physics in 1992 and 1997, respectively, from the University of Notre Dame, Notre Dame, IN, where he helped develop a particle tracking system using organically doped polymer optical fibers.

In 1998, he joined Lucent Technologies, Bell Laboratories, Murray Hill, NJ, as a Member of Technical Staff. He currently works on novel SOA-based integrated components and high-power optical fiber amplifiers.

S. S. Patel was born in Bombay, India, in 1960. He received the Bachelor of Technology degree in chemical engineering from the Indian Institute of Technology, IIT Kanpur, India, in 1982 and the Ph.D. degree in chemical engineering and materials science from the University of Minnesota in 1988.

He joined Bell Laboratories, Holmdel, NJ, in 1988. His work at Bell Laboratories has spanned many disciplines, including polymer morphology, colloidal dynamics, photonics band-gap materials, radio frequency absorption from cellular handsets in humans, and holographic storage. He is currently working on waveguide devices for optical networking.